parameter, using the F-distributed model test statistic [equation 20 of R. A. Bennett, W. Rodi, R. E. Reilinger *J. Geophys. Res.* **101**, 21943 (1996)]. This test allows us to assess the level of complexity in the deformation model required to explain the baseline time series.
18. See C. H. Scholz, *The Mechanics of Earthquakes and Faulting* (Cambridge Univ. Press, Cambridge, 1990), chaps. 4 and 5, and references therein.
19. J. L. Davis, T. A. Herring, I. I. Shapiro, A. E. E. Rogers, G. Elgered, *Radio Sci.* **20**, 1593 (1985).
20. If the error sources serendipitously resulted in the observed χ^2 per degree of freedom of slightly less than unity (*12*), the "true" χ^2 per degree of freedom would be significantly less than unity.
21. The average rate across the entire Basin and Range is ~15 to 20 nstr/year [for example, T. H. Dixon, S. Robaudo, J. Lee, M. C. Reheis, *Tectonics* **14**, 755 (1995); R. A. Bennett, B. P. Wernicke, J. L. Davis, *Geophys. Res. Lett.* **25**, 563 (1998)]. Rates of ~200 nstr/year are typical along the San Andreas fault [for example, W. Thatcher, *U.S. Geol. Surv. Prof. Pap. 1515* (1990)], p. 189.
22. R. E. Wallace, *J. Geophys. Res.* **89**, 5763 (1984); R. S. Stein, S. E. Barrientos, *ibid.* **90**, 11355 (1985); M. N. Machette, S. F. Personius, A. R. Nelson, *Ann. Tectonic.* **6** (suppl.), 5 (1992).
23. T. Parsons and G. A. Thompson, *Science* **253**, 1399 (1991).
24. J. R. Evans and M. Smith III, in *Major Results of Geophysical Investigations at Yucca Mountain and Vicinity, Southern Nevada*, H. W. Oliver, D. A. Ponce, W. Clay Hunter, Eds. [Open-File Report, U.S. Geological Survey, OF-0074 (1995)], pp. 135–156.
25. P. T. Delaney and A. E. Gartner, *Geol. Soc. Am. Bull.* **109**, 1177 (1997).
26. R. E. Wallace, *Bull. Seismol. Soc. Am.* **77**, 868 (1987).
27. E. I. Smith, D. L Feuerbach, T. R. Nauman, J. E. Faulds, *Proceedings of the International Topical Meeting, High-Level Radioactive Waste Management* (American Nuclear Society/American Society of Civil Engineers, Las Vegas, 1990), vol. 1, pp. 81–90.
28. We thank J. Savage and M. Lisowski for providing trilateration data and GPS data and results from their 1993 survey, and J. Savage for useful discussions. The University NAVSTAR Consortium provided equipment and field logistical support. This project was funded by Nuclear Regulatory Commission contracts NRC-04-92-071 and NRC-02-93-005, and National Science Foundation grant EAR-94-18784.

29 October 1997; accepted 3 March 1998

Test of General Relativity and Measurement of the Lense-Thirring Effect with Two Earth Satellites

Ignazio Ciufolini, Erricos Pavlis, Federico Chieppa, Eduardo Fernandes-Vieira, Juan Pérez-Mercader

The Lense-Thirring effect, a tiny perturbation of the orbit of a particle caused by the spin of the attracting body, was accurately measured with the use of the data of two laser-ranged satellites, LAGEOS and LAGEOS II, and the Earth gravitational model EGM-96. The parameter μ, which measures the strength of the Lense-Thirring effect, was found to be 1.1 ± 0.2; general relativity predicts $\mu \equiv 1$. This result represents an accurate test and measurement of one of the fundamental predictions of general relativity, that the spin of a body changes the geometry of the universe by generating space-time curvature.

Einstein's general theory of relativity (*1*, *2*) predicts the occurrence of peculiar phenomena in the vicinity of a spinning body, caused by its rotation, that have not yet been measured (*3*). When a clock that co-rotates very slowly around a spinning body returns to its starting point, it finds itself advanced relative to a clock kept there at "rest" (with respect to "distant stars"). Indeed, synchronization of clocks all around a closed path near a spinning body is not possible, and light co-rotating around a spinning body would take less time to return to a fixed point than light rotating in the opposite direction (*2*). Similarly, the orbital period of a particle co-rotating around a spinning body would be longer than the orbital period of a particle counter-rotating on the same orbit. Furthermore, an orbiting particle around a spinning body will have its orbital plane "dragged" around the spinning body in the same sense as the rotation of the body, and small gyroscopes that determine the axes of a local, freely falling, inertial frame, where "locally" the gravitational field is "unobservable," will rotate with respect to "distant stars" because of the rotation of the body. This phenomenon—called "dragging of inertial frames" or, more simply, "frame dragging," as Einstein named it—is also known as the Lense-Thirring effect (*1*, *2*, *4*). In Einstein's general theory of relativity, all of these phenomena are the result of the rotation of the central mass.

Rotation, inertia, and the "fictitious" inertial forces arising in a rotating system have been central issues and problems of mechanics since the time of Galileo and Newton (*5*). Mach thought that the centrifugal forces were the result of rotation with respect to the masses in the universe, and Einstein's development of the general theory of relativity was influenced by Mach's ideas on the origin of inertia and inertial forces. Today, the level at which general relativity satisfies Mach's ideas on inertia is still debated and discussed. However general relativity satisfies at least a kind of "weak manifestation" of Mach's ideas: the dragging of inertial frames (*2*). Indeed, in Einstein's gravitational theory, the concept of an inertial frame has only a local meaning, and a local inertial frame is "rotationally dragged" by mass-energy currents because moving masses influence and change the orientation of the axes of a local inertial frame (that is, the gyroscopes); thus, a current of mass such as the spinning Earth "drags" and changes the orientation of the gyroscopes with respect to the distant stars.

To understand these phenomena of general relativity associated with the rotation of a mass, one may use a formal analogy with the classical theory of electromagnetism. Newton's law of gravitation has a formal counterpart in Coulomb's law of electrostatics; however, Newton's theory has no phenomenon formally analogous to magnetism. On the other hand, Einstein's theory of gravitation predicts that the force generated by a current of electrical charge, described by Ampere's law, should also have a formal counterpart "force" generated by a current of mass. The detection and measurement of this "gravitomagnetic" force is the subject of this report.

The gravitomagnetic force causes a gyroscope to precess with respect to an asymptotic inertial frame with angular velocity $\dot{\Omega} = -\frac{1}{2}\mathbf{H} = [-\mathbf{J} + 3(\mathbf{J}\cdot\hat{\mathbf{x}})\hat{\mathbf{x}}]/|\mathbf{x}|^3$, where $\mathbf{H}$ is the gravitomagnetic field, $\mathbf{J}$ is the angular momentum of the central object, and $\mathbf{x}$ is the gyroscope's position vector. This formula quantifies the Lense-Thirring effect for a gyroscope (*1*, *2*). The gravitomagnetic force also causes small changes in the orbit of a test particle (*4*). In particular, there is a secular rate of change of the longitude of the nodes (intersection between the orbital plane of the test particle and the equatorial plane of the central object) given by $\dot{\Omega}^{\text{Lense-Thirring}} = 2\mathbf{J}/[a^3(1 - e^2)^{3/2}]$, where a is the semimajor axis of the test particle's orbit and e is its orbital eccentricity. In addition, there is a secular rate of change of the longitude of the pericenter (*2*), $\tilde{\omega}$ (determined by the Runge-Lenz vector): $\dot{\tilde{\omega}}^{\text{Lense-Thirring}} = 2J[\hat{\mathbf{J}} -$

I. Ciufolini, Istituto Fisica Spazio Interplanetario–Consiglio Nazionale delle Ricerche, and Dipartimento Aerospaziale, Universitá di Roma "La Sapienza," via Eudossiana 16, 00184 Rome, Italy.
E. Pavlis, Joint Center for Earth System Technology, University of Maryland–Baltimore County, Baltimore, MD 21250, USA.
F. Chieppa, Scuola Ingegneria Aerospaziale, Universitá di Roma "La Sapienza," Rome, Italy.
E. Fernandes-Vieira and J. Pérez-Mercader, Laboratorio de Astrofisica Espacial y Fisica Fundamental (INTA-CSIC), Madrid, Spain.

$3(\cos I)\hat{\mathbf{l}}]/[a^3(1 - e^2)^{3/2}]$, where I is the orbital inclination, $\cos I \equiv \hat{\mathbf{J}}\cdot\hat{\mathbf{l}}$, and $\mathbf{l}$ is the particle's orbital angular momentum (Fig. 1).

In astrophysics, a supermassive spinning black hole and its gravitomagnetic field may explain the constant orientation of the long jets of matter ejected from the cores of quasars and active galactic nuclei (*6*). These jets have emission times that may reach millions of years.

Here we describe a direct measurement, with an accuracy of about 20%, of one of the phenomena caused by the gravitomagnetic field (*4*). Our detection and measurement was obtained by using the satellite laser-ranging (*7*) data of the satellites LAGEOS (Laser Geodynamics Satellite, NASA) and LAGEOS II [NASA and the Italian space agency (ASI)] and the latest Earth gravitational field model, EGM-96.

The measurement of distances has always been a fundamental issue in astronomy, engineering, and science in general. So far, laser ranging has been the most accurate technique for measuring the distances to the moon and artificial satellites (*7*). Short-duration laser pulses are emitted from lasers on Earth, aimed at the target through a telescope, and then reflected back by optical cube-corner retroreflectors on the moon (*8*) or the artificial satellite (*9*), such as LAGEOS (*10*). By measuring the total round-trip travel time, one can determine the distance to a retroreflector on the moon with an accuracy of about 2 cm and to the LAGEOS satellites with a few millimeters accuracy.

We analyzed the laser-ranging data using the principles described in (*11*) and adopted the IERS conventions (*12*) in our modeling, except that we used the recently released static and tidal EGM-96 model (*13*). Error analysis of the LAGEOS orbits indicated that the EGM-96 errors can only contribute periodic root-sum-square errors of 2 to 4 mm radially, and in all three directions they do not exceed 10 to 17 mm. The initial positions and velocities of the LAGEOS satellites were adjusted for each 15-day batch of data, along with a set of accelerations in the along-track direction (to account for the residual drag at the satellites' altitude) and small variations in their reflectivities. Solar radiation pressure, Earth albedo, and anisotropic thermal effects were also modeled (*14*). In modeling the thermal effects, the orientation of the satellite spin axis was obtained from (*15*). Lunar, solar, and planetary perturbations were also included in the equations of motion, formulated according to Einstein's general theory of relativity with the exception of the Lense-Thirring effect, which was purposely set to zero. All of the tracking station coordinates were adjusted (accounting for tectonic motions) except for those defining the TRF terrestrial reference frame. Polar motion was also adjusted, and Earth's rotation was modeled from the very long baseline interferometry–based series SPACE96 (*16*). We analyzed the orbits of the LAGEOS satellites using the orbital analysis and data reduction software GEODYN II (*17*).

The node and perigee of LAGEOS and LAGEOS II (Fig. 1) are dragged by Earth's angular momentum. From the Lense-Thirring formula, we get $\dot{\Omega}_{\mathrm{I}}^{\text{Lense-Thirring}} \approx 31$ mas/year and $\dot{\Omega}_{\mathrm{II}}^{\text{Lense-Thirring}} \approx 31.5$ mas/year, where mas is a millisecond of arc. The argument of pericenter (perigee in our analysis) ω of a test particle—that is, the angle on its orbital plane that measures the departure of the pericenter from the equatorial plane of the central body—also has a Lense-Thirring drag: $\dot{\omega}_{\mathrm{I}}^{\text{Lense-Thirring}} \approx 32$ mas/year and $\dot{\omega}_{\mathrm{II}}^{\text{Lense-Thirring}} \approx -57$ mas/year. The nodal precessions of LAGEOS and LAGEOS II can be determined with an accuracy of the order of 1 mas/year. Over our total observational period of about 4 years, we obtained a root mean square of the node residuals of ~4 mas for LAGEOS and ~7 mas for LAGEOS II. For the perigee, the observable quantity is the product $ea\dot{\omega}$. The perigee precession $\dot{\omega}$ for LAGEOS is difficult to measure because its orbital eccentricity $e \approx 0.004$. The orbit of LAGEOS II is more eccentric, with $e \sim 0.014$, and the Lense-Thirring drag of the perigee of LAGEOS II is almost twice as large in magnitude as that of LAGEOS. Over about 4 years, we obtained a root mean square of the residuals of the LAGEOS II perigee of about 25 mas, whereas the total Lense-Thirring effect on the perigee is, over 4 years, ≈ -228 mas. To measure the Lense-Thirring effect from the residuals of the orbital elements, we introduced a parameter μ, which, by definition, is equal to one in general relativity (*2*) and zero in Newtonian theory.

The main error in this measurement is due to the uncertainties in Earth's even zonal harmonics and their time variations. The unmodeled orbital effects due to the harmonics of lower order are comparable to, or larger than, the Lense-Thirring effect. However, by analyzing the EGM-96 model with its uncertainties in the even zonal harmonic coefficients, and by calculating the secular effects of these uncertainties on the orbital elements of LAGEOS and LAGEOS II, we find that the main sources of error in the determination of the Lense-Thirring effect are concentrated in the first two even zonal harmonics, J_2 and J_4. We can, however, use the three observable quantities $\dot{\Omega}_{\mathrm{I}}$, $\dot{\Omega}_{\mathrm{II}}$, and $\dot{\omega}_{\mathrm{II}}$ to determine μ (*18*), thereby avoiding the two largest sources of error, those arising from the uncertainties in J_2 and J_4. We do this by solving the system of the three equations for $\delta\dot{\Omega}_{\mathrm{I}}$, $\delta\dot{\Omega}_{\mathrm{II}}$, and $\delta\dot{\omega}_{\mathrm{II}}$ in the three unknowns μ, J_2, and J_4, obtaining

$$\delta\dot{\Omega}_{\mathrm{I}}^{\mathrm{Exp}} + c_1\delta\dot{\Omega}_{\mathrm{II}}^{\mathrm{Exp}} + c_2\delta\dot{\omega}_{\mathrm{II}}^{\mathrm{Exp}} = \mu(31 + 31.5c_1 - 57c_2)\ \text{mas/year} + \text{other errors} \approx \mu(60.2\ \text{mas/year}) \quad (1)$$

where $c_1 = 0.295$ and $c_2 = -0.35$. Equation 1 for μ does not depend on J_2 and J_4 nor on their uncertainties; thus, the value of μ that we obtain is unaffected by the largest errors, which are due to δJ_2 and δJ_4, and is sensitive only to the smaller errors due to δJ_{2n} with $2n \geq 6$.

Similarly, regarding tidal, secular, and seasonal changes in the geopotential coefficients, the main effects on the nodes and perigee of LAGEOS and LAGEOS II, caused by tidal and other time variations in Earth's gravitational field (*19, 20*), are due to changes in J_2 and J_4. However, the tidal errors in J_2 and J_4 and the errors resulting

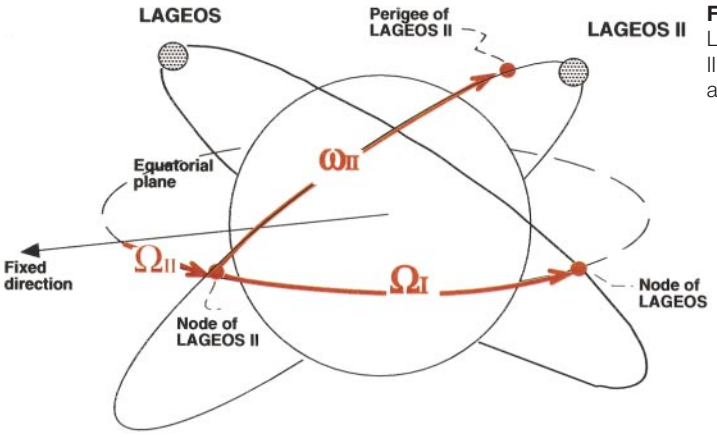

Fig. 1. The orbits of LAGEOS and LAGEOS II; their nodes Ω_{I} and Ω_{II}; and perigee ω_{II}.

from other unmodeled time variations in J_2 and J_4, including their secular and seasonal variations, are eliminated by our combination of residuals of nodes and perigee. In particular, most of the errors resulting from the 18.6- and 9.3-year tides, associated with the lunar node, are eliminated in our measurement. The same method was used in (*20*), but the gravitational field model and especially the Earth tidal model used here are more accurate. Also, we refined the nongravitational perturbations model, and the total period of observation was here longer by 1 year. Thus, we substantially reduced the total error in the measurement of μ. An extensive discussion of the various error sources that can affect the result is given in (*20*); only a brief discussion of the error sources is given here.

In Fig. 2, we display the linear combination of the residuals of the nodes of LAGEOS and LAGEOS II and perigee of LAGEOS II according to Eq. 1 to eliminate the δJ_2 and δJ_4 errors after removing four small periodic residual signals and the small observed inclination residuals. The removal of the periodic terms was achieved by a least squares fit of the residuals using a secular trend and four periodic signals with 1044-, 820-, 569-, and 365.25-day periods, corresponding to, respectively, the nodal period of LAGEOS, the perigee and nodal periods of LAGEOS II, and 1 year. The 820-day period is the period of the main odd zonal harmonics perturbations of the LAGEOS II perigee; the 1044- and 569-day periods are the periods of the main tidal orbital perturbations, with $l = 2$ and $m = 1$, which were not eliminated using Eq. 1. Some combinations of these frequencies correspond to the main nongravitational perturbations of the LAGEOS II perigee. We stress that the present analysis using EGM-96 and its accurate tidal model is substantially independent of the removed signals, whereas the previous analysis (*20*) depended on the periodic terms included in the fit. In other words, our value (Fig. 2) of the secular trend does not significantly change by fitting additional periodic perturbations, and indeed, even the fit of the residuals with a secular trend only, with no periodic terms, just increases the slope by less than 10%. Nevertheless, in this case, the root mean square of the post-fit residuals increases by about four times with respect to Fig. 2.

Our best-fit straight line of Fig. 2, through the combined residuals of nodes and perigee, has a slope $\mu_{meas} \approx 1.1 \pm 0.03$, where 0.03 is its standard deviation. This combined, measured, gravitomagnetic perturbation of the satellites' orbits corresponds to about 16 m at the LAGEOS altitude, that is, about 265 mas. The root mean square of the post-fit combined residuals is about 9 mas. Our total error is reduced to 20% of μ_{GR}. Using the EGM-96 covariance matrix, we found the errors due to uncertainties in the even zonal harmonics J_{2n} with $2n \geq 6$ to be $\delta\mu_{even} \lesssim 13\%$ of μ_{GR}, and the errors in the modeling of the perigee rate of LAGEOS II due to uncertainties in the odd zonal harmonics J_{2n+1}, $\delta\mu_{odd} \lesssim 2\%$ of μ_{GR}. Using the improved tidal model, we estimated the effect of tidal perturbations and other variations of Earth gravitational field to be $\delta\mu_{tides} \lesssim 4\%$ of μ_{GR}. On the basis of analyses (*20*) of the nongravitational perturbations—in particular, those on the perigee of LAGEOS II—we found $\delta\mu_{nongrav} \lesssim 13\%$ of μ_{GR}, and the error due to uncertainties in the orbital inclinations of LAGEOS and LAGEOS II was estimated as $\delta\mu_{incl} \lesssim 5\%$ of μ_{GR}. Taking into account all of these error sources, we arrived at a total root-sum-square error $\lesssim$20% of μ_{GR}. Therefore, over an observational period of 4 years and using EGM-96, we determined $\mu_{meas} = 1.1 \pm 0.2$, where 0.2 is the estimated total uncertainty due to all of the error sources.

Based on the analysis of the orbits of the laser-ranged satellites LAGEOS and LAGEOS II, we conclude that the gravitomagnetic or Lense-Thirring effect exists, and its value is within 10%, plus or minus a total error of 20%, of what is predicted by Einstein's theory of general relativity, that is, $\mu_{GR} = 1$. Hence, this direct measurement of the Lense-Thirring effect confirms one of the remaining fundamental predictions of general relativity, that a current of mass-energy, such as a spinning mass, as a result of its mass-motion, changes the geometry of the universe (*2*) by generating space-time curvature.

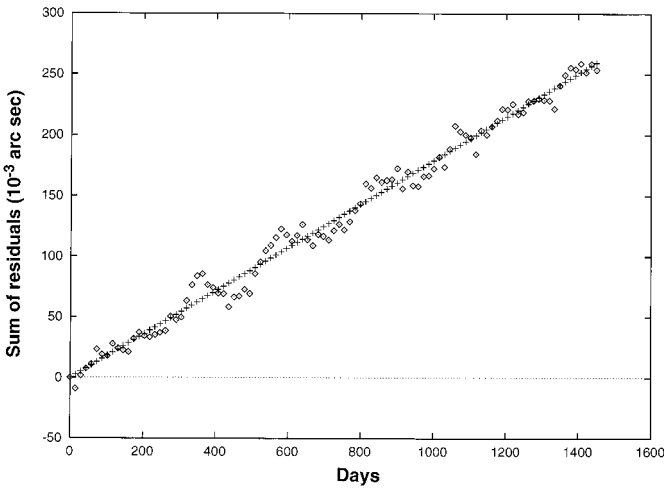

Fig. 2. Sum of the residuals (diamonds) of the nodes of LAGEOS and LAGEOS II and perigee from January 1993 to January 1997. On the vertical axis, we plotted (node residuals of LAGEOS) + 0.295(node residuals of LAGEOS II) − 0.35(perigee residuals of LAGEOS II). The best-fit line (crosses) shown through these combined residuals has a slope of about 66 mas/year (mas is a millisecond of arc; the total integrated effect corresponds to about 16 m at the LAGEOS altitude); that is, $\mu_{meas} \approx 1.1$ (compared with $\mu^{GR} \equiv 1$ in general relativity). The standard deviation of the slope is about 2 mas/year, and the root mean square of the post-fit residuals is about 9 mas. Because of modeling errors (secular and periodic) and random errors, we estimate the total error in our measurement of μ to be $\lesssim$20% of μ.

REFERENCES AND NOTES

1. C. W. Misner, K. S. Thorne, J. A. Wheeler, *Gravitation* (Freeman, San Francisco, 1973).
2. I. Ciufolini and J. A. Wheeler, *Gravitation and Inertia* (Princeton Univ. Press, Princeton, NJ, 1995).
3. A direct observation of the Lense-Thirring effect using the LAGEOS and LAGEOS II satellites was obtained in 1995 [I. Ciufolini *et al.*, *Nuovo Cimento A* **109**, 579 (1996)]. However, the total observational period of this analysis was quite short, and the perturbations model was less accurate than the one used in the measurement reported in (*20*). Because of the refined perturbations models and the longer period of observation, the present work is the first accurate direct measurement of the Lense-Thirring effect using the LAGEOS satellites. An indirect astrophysical observation of frame-dragging was obtained in 1988 using the periastron precession rate of the binary pulsar PSR 1913+16 [K. Nordtvedt, *Int. J. Theor. Phys.* **27**, 1395 (1988)]. Recent analyses of galactic sources of x-rays may represent another astrophysical observation of this effect in the accretion disks of black holes and neutron stars [W. Cui *et al.*, *Astrophys. J.* **492**, L53 (1998)].
4. J. Lense and H. Thirring, *Phys. Z.* **19**, 156 (1918) [English translation by B. Mashhoon, F. W. Hehl, D. S. Theiss, *Gen. Relativ. Gravitation* **16**, 711 (1984)].
5. In Newton's famous gedanken experiment of a rotating bucket filled with water, the question was "which is the origin of the inertial forces that curve the surface of the water in the bucket? Are these forces produced by the relative rotation of the bucket with respect to absolute space or with respect to the other masses of the universe?"
6. K. S. Thorne, R. H. Price, D. A. MacDonald, Eds., *Black Holes: The Membrane Paradigm* (Yale Univ. Press, New Haven, CT, 1986).
7. S. C. Cohen *et al.*, Eds., *J. Geophys. Res.* **90** (no. B11), 9215–9438 (1985); P. Bender and C. C. Goad, in *Proceedings of the Second International Symposium on the Use of Artificial Satellites for Geodesy and Geodynamics*, G. Veis and E. Livieratos, Eds. (National Technical University, Athens, 1979), pp. 145–161.
8. K. Nordtvedt, *Phys. Today* **49**, 26 (May 1996).
9. J. J. Degnan and E. C. Pavlis, *GPS World* **5**, 62 (1994).

10. The LAGEOS satellites are heavy brass and aluminum satellites, of about 406 kg, completely passive and covered with retroreflectors, orbiting about 6000 km above Earth's surface. LAGEOS, launched in 1976 by NASA, and LAGEOS II, launched by NASA and ASI in 1992, have an essentially identical structure but are in different orbits. The semimajor axis of LAGEOS is $a_I \approx 12{,}270$ km, the period $P_I \approx 3.758$ hours, the eccentricity $e_I \approx 0.004$, and the inclination $I_I \approx 109.9°$. For LAGEOS II, $a_{II} \approx 12{,}163$ km, $e_{II} \approx 0.014$, and $I_{II} \approx 52.65°$.
11. *International Earth Rotation Service* (*IERS*) *Annual Report, 1996* (Observatoire de Paris, Paris, July 1997).
12. D. McCarthy, *The 1996 IERS Conventions* (Observatoire de Paris, Paris, 1996).
13. F. G. Lemoine *et al.*, presented at the 1997 Institute of Astronomy and Geophysics Scientific Assembly, Rio de Janeiro, Brazil, 5 to 9 September 1997.
14. D. P. Rubincam, *J. Geophys. Res.* **93**, 13803 (1988); *ibid.* **95**, 4881 (1990); _____ and A. Mallama, *ibid.* **100**, 20285 (1995); C. F. Martin and D. P. Rubincam, *ibid.* **101**, 3215 (1996).
15. P. Farinella, D. V. Y. Vokrouhlicky, F. Barlier, *ibid.*, 17861.
16. R. S. Gross, *ibid.*, p. 8729.
17. D. E. Pavlis *et al.*, *GEODYN II: Operations Manual* (1997), vol. 3.
18. I. Ciufolini, *Phys. Rev. Lett.* **56**, 278 (1986); *Nuovo Cimento A* **109**, 1709 (1996).
19. _____, *Int. J. Mod. Phys. A* **4**, 3083 (1989); see also B. Tapley, J. C. Ries, R. J. Eanes, M. M. Watkins, *NASA-ASI Study on LAGEOS III* (1989), part A, I. Ciufolini *et al.*; *ibid.*, part B.
20. I. Ciufolini *et al.*, *Classical Quantum Gravity* **14**, 2701 (1997).
21. This work was significantly aided by several programs and facilities of NASA Goddard Space Flight Center (GSFC), in particular through data provided to us by the Crustal Dynamics Data and Information System (CDDIS) of NASA GSFC and the use of the program GEODYN II. We also appreciate unconditional help from D. E. Pavlis and D. D. Rowlands. I.C. and F.C. were supported in part by ASI, E.F.-V. and J.P.-M. by the Ministries of Education and Defense of Spain, and E.P. in part by NASA grant NCC-5-60.

28 October 1997; accepted 12 February 1998

Quantitation of HIV-1–Specific Cytotoxic T Lymphocytes and Plasma Load of Viral RNA

Graham S. Ogg, Xia Jin, Sebastian Bonhoeffer, P. Rod Dunbar, Martin A. Nowak, Simon Monard, Jeremy P. Segal, Yunzhen Cao, Sarah L. Rowland-Jones, Vincenzo Cerundolo, Arlene Hurley, Martin Markowitz, David D. Ho, Douglas F. Nixon, Andrew J. McMichael*

Although cytotoxic T lymphocytes (CTLs) are thought to be involved in the control of human immunodeficiency virus–type 1 (HIV-1) infection, it has not been possible to demonstrate a direct relation between CTL activity and plasma RNA viral load. Human leukocyte antigen–peptide tetrameric complexes offer a specific means to directly quantitate circulating CTLs ex vivo. With the use of the tetrameric complexes, a significant inverse correlation was observed between HIV-specific CTL frequency and plasma RNA viral load. In contrast, no significant association was detected between the clearance rate of productively infected cells and frequency of HIV-specific CTLs. These data are consistent with a significant role for HIV-specific CTLs in the control of HIV infection and suggest a considerable cytopathic effect of the virus in vivo.

At all stages of disease, plasma RNA viral load remains the most potent predictor of outcome in HIV-1–infected individuals (*1*). Cross-sectional stratification of RNA loads provides a highly significant indicator of the likelihood of progression to acquired immunodeficiency syndrome (AIDS) and mortality (*1*). Even shortly after seroconversion the virological setpoint is significantly associated with prognosis, suggesting that in most individuals the determinants of progression are present early in the course of infection (*1*). The dominant host immunological factors involved in the control of progression remain unresolved, but most infected individuals show a vigorous HIV-specific immune response comprising both cellular and humoral mechanisms.

Cytotoxic T lymphocytes (CTLs) are believed to be important in the control of HIV infection (*2*–*6*) because the emerging HIV-specific CTL response observed during primary infection follows a close temporal association with acute viral load reduction (*2*, *3*). Evidence also comes from the characterization of virus mutants that escape recognition by CTLs that have been identified at seroconversion, during asymptomatic HIV infection, during AIDS, and after CTL immunotherapy (*4*, *5*), suggesting that CTLs exert a considerable selective pressure at many stages of disease. In addition to killing infected cells, $CD8^+$ T cells effectively inhibit HIV replication in vitro through the production of chemokines (*6*).

Mathematical modeling of viral dynamics has predicted that if CTLs are important in the control of HIV infection, there should be an inverse association between HIV-specific CTL activity and plasma RNA viral load (*7*, *8*). However, previous studies have demonstrated no significant correlation between circulating HIV-specific CTL activity and plasma RNA viral load during the chronic phase (*9*–*11*). High CTL activity in the presence of low levels of plasma viral RNA has been reported, but these findings were based on qualitative associations and indirect assays of CTL function that require culture and expansion in vitro (*12*). In a study of early HIV infection only, the levels of Env-specific cultured memory CTLs were inversely correlated with RNA viral load, but this finding did not extend to Gag- or Pol-specific memory CTLs (*13*). Direct measurement of lytic activity by uncultured, circulating HIV-specific CTLs (effector CTLs, CTLe) has only been possible in a subset of patients because the assay is relatively insensitive, requiring antigen-specific CTLe frequencies above 1 in 100 peripheral blood mononuclear cells (PBMCs) for lysis to be detectable (*14*). Here we have used highly sensitive human leukocyte antigen (HLA)–tetrameric complexes for a cross-sectional analysis of HIV Gag- and Pol-specific CTLe frequencies from 14 untreated HLA A*0201–positive individuals at different stages of infection.

HLA-tetrameric complexes can be used to directly visualize antigen-specific T cells by flow cytometry (*15*). HLA heavy chain is expressed in *Escherichia coli* with an engineered COOH-terminal signal sequence containing a biotinylation site for the enzyme BirA (*16*). After refolding of heavy chain, β_2-microglobulin (β_2M), and peptide, the complex is biotinylated and tetramer formation induced by the addition of streptavidin. By means of fluorescently labeled streptavidin, the tetramer can be used to stain and sort antigen-specific cells. The staining is highly specific such that CTL clones and lines directed to different epitope peptides bound to the same HLA molecule do not stain (*15*). Figure 1, A to C, shows examples of HLA-tetrameric staining with (A) HLA B*3501 tetramer refolded around the envelope peptide DPNPQEVVL [Env(77–85)] (*17*), (B) HLA

G. S. Ogg, P. R. Dunbar, S. L. Rowland-Jones, V. Cerundolo, A. J. McMichael, Institute of Molecular Medicine, Nuffield Department of Medicine, Oxford OX3 9DS, UK.
X. Jin, S. Monard, J. P. Segal, Y. Cao, A. Hurley, M. Markowitz, D. D. Ho, D. F. Nixon, Aaron Diamond AIDS Research Center, 455 First Avenue, New York, NY 10016, USA.
S. Bonhoeffer, Aaron Diamond AIDS Research Center, 455 First Avenue, New York, NY 10016, USA, and Department of Zoology, University of Oxford, South Parks Road, Oxford OX13PS, UK.
M. A. Nowak, Department of Zoology, University of Oxford, South Parks Road, Oxford OX1 3PS, UK.
*To whom correspondence should be addressed.